Molecular Crystals and Liquid Crystals Science and Technology. Section A. Molecular Crystals and Liquid Crystals

Publication details, including instructions for authors and subscription information:
http://www.tandfonline.com/loi/gmcl19

Heterojunctions, Quantum Confinement, and Electronic Competitions in Mixed Halide MX Solids

S. P. Love [a] , B. Scott [a] , X. Z. Huang [a] , A. Saxena [a] , A. R. Bishop [a] & B. I. Swanson [a]

[a] Los Alamos National Laboratory, LOS Alamos, New Mexico, 87545, U.S.A.

Version of record first published: 04 Oct 2006.

To cite this article: S. P. Love , B. Scott , X. Z. Huang , A. Saxena , A. R. Bishop & B. I. Swanson (1994): Heterojunctions, Quantum Confinement, and Electronic Competitions in Mixed Halide MX Solids, Molecular Crystals and Liquid Crystals Science and Technology. Section A. Molecular Crystals and Liquid Crystals, 256:1, 171-178

To link to this article: http://dx.doi.org/10.1080/10587259408039245

Mol. Cryst. Liq. Cryst. 1994, Vol. 256, pp. 171–178
Reprints available directly from the publisher
Photocopying permitted by license only

HETEROJUNCTIONS, QUANTUM CONFINEMENT, AND ELECTRONIC COMPETITIONS IN MIXED HALIDE MX SOLIDS

S. P. LOVE, B. SCOTT, X. Z. HUANG, A. SAXENA,
A. R. BISHOP and B. I. SWANSON
Los Alamos National Laboratory,
Los Alamos, New Mexico, 87545 U.S.A.

Abstract The mixed-halide MX solids $[Pt(en)_2][Pt(en)_2(X_yX'_{1-y})_2](ClO_4)_4$ (X,X'=Cl, Br, or I; en=1,2-diaminoethane) -- abbreviated PtX1-yX'y -- are realizations of nanoscale 1-D heterostructures in a well-characterized crystalline environment. Using resonance Raman spectroscopy, the complex interplay between quantum confinement, lattice mismatch effects, charge transfer at heterojunctions, and electronic interaction lengths across the junctions is explored for two CDW strength combinations: the strong-/moderate-CDW case of $PtCl_{1-x}Br_x$ the strong-/weak-CDW case of $PtCl_{1-x}I_x$.

INTRODUCTION

The quasi-one-dimensional halogen-bridged transition metal chain solids (MX materials) continue to prove their value as model systems for detailed theoretical and experimental exploration of the electronic behavior of materials with restricted dimensionality. These crystalline solids are composed of chains of alternating metal (M=Pt, Pd, or Ni) and halogen (X=Cl,Br, or I) atoms. Typically the metals are equatorially coordinated by amine ligands, and counterions between the chains complete the crystal structure. Usually the MX chains are Peierls distorted, with an accompanying charge density wave (CDW) on the metals.

MX solids make excellent model materials because they can be tuned over a wide range -- from the non-distorted spin density wave regime to a highly distorted Peierls insulator with a band gap of 3.2 eV -- simply through the choice of metal, halogen, ligand and counterion. Furthermore, their simplicity and highly 1-D nature makes them particularly amenable to theoretical modeling. Models based on a 2-band 3/4-filled Peierls-Hubbard (P-H) Hamiltonian

have been highly successful in predicting electronic and vibrational properties of the MX materials.[1]

The range of 1-D phenomena for which the MX solids serve as useful prototypes is greatly extended through the study of mixed-halide $MX_{1-y}X'_y$ solids. We have found that many such mixtures, rather than phase-segregating into domains of MX and MX', actually form high-quality single crystals made up of quasi-infinite chains comprised of interspersed MX and MX' segments of varying length. Apart from the disorder of the X and X' ions within these mixed chains, long-range crystalline order is maintained.

The outstanding aspect of these mixed crystals is that the mixed chains, with their MX and MX' segments spliced end-to-end, provide self-assembled collections of 1-D heterojunctions and molecular-scale 1-D quantum wells. With the great tunability of the MX class, this provides an extraordinary opportunity to study such structures for a variety of combinations of CDW strengths (i.e., band gaps), all in a well-characterized crystalline environment.

Typical questions which arise regarding such 1-D heterostructures include the following: (1) In crossing a junction from MX into MX', how far into the MX' segment does the presence of the junction result in a perturbation of the MX' band structure -- i.e. what is the electronic healing length? (2) Is there charge transfer across junctions, analogous to Schottky barrier formation? (3) How does quantum confinement affect the electronic and vibrational energies for various segment lengths?

All of these questions can be addressed through resonance Raman (RR) spectroscopy given a sufficient theoretical knowledge of the system. The basic difficulty with the $MX_{1-y}X'_y$ mixed crystals is that they consist of complex distributions of MX and MX' segment lengths in many configurations, resulting in complex spectra which initially may appear intractable. The great strength of RR spectroscopy, however, is its ability to selectively probe the various types of segments and junctions by tuning the excitation laser to their particular resonance energies, thus identifying the electronic and vibrational energies of those segments. This information, together with knowledge of relative segment lengths gained by varying the X' fraction and from isotopic substitutions, can be used in the P-H model to generate a relatively complete picture of these systems. In this article we use this process to compare two strikingly different MXX' systems of the form $[Pt(en)_2][Pt(en)_2(X_yX'_{1-y})_2](ClO_4)_4$, the first with X=Cl and X'=Br (a strong-/moderate-CDW combination), and the second

with X=Cl and X'=I (a strong-/weak-CDW combination). Henceforth we shall abbreviate these as "$PtCl_{1-x}Br_x$" and "$PtCl_{1-x}I_x$".

LATTICE DYNAMICS CONSIDERATIONS

The first aspect of the mixed chains which must be realized is that the halide disorder destroys the translational symmetry of the chains, resulting in highly localized vibrational modes rather than extended phonons. This has been discussed in detail elsewhere,[2] so here we provide only a brief summary.

In the MXX' chains these localized modes fall into three general categories. First, there are the modes localized on MX chain segments, terminated by MX' segments. Here the vibrational amplitude is almost entirely confined to the MX segment, with very small participation from a few MX' atoms near the junction. The most strongly Raman-active versions of these modes will be those in which all the cells of the MX segment move in phase. To intuitively predict the frequencies of these segment modes, one can think of them, very crudely, as being like a 1/2-wave piece of an extended phonon of wave vector π/L where L is the segment length. Since the Raman-active phonon branch (ν_1) of MX chains always increases in frequency with increasing wave vector, it is clear that (in the absence of electronic effects that could lead to L-dependent spring constants) shorter segments will have higher Raman frequencies.

The second class of local mode in the MXX' chains are modes localized at the junctions, with the vibrational amplitude concentrated on the X-M-X' "molecule" forming the junction. Finally, under some circumstances (in particular for the $PtCl_{1-x}I_x$ chains) the vibrational localization length for segment modes is long enough that nearby but non-adjacent MX segments couple to each other through the intervening MX' segment, giving rise to a complicated third class of local mode having vibrational amplitude spread over several MX and MX' segments.

THE CHLORIDE/BROMIDE MIXED SYSTEM

These lattice dynamics effects are seen in their simplest form in the RR spectra of the $PtCl_{1-x}Br_x$ system. These RR results and their interpretation were described in detail elsewhere for this strong-/moderate-CDW strength combination;[3] we summarize them here for later comparison with the strong-/weak-CDW $PtCl_{1-x}I_x$ system. In the

$PtCl_{1-x}Br_x$ system, the 165.5 cm^{-1} ν_1 mode of pure PtBr is replaced by a series of sharp lines at frequencies ν_n ranging from 167 to 181 cm^{-1}. In this series, each higher ν_n mode is resonantly enhanced at successively higher excitation energies (ranging from ~1.6 eV for the 167 cm^{-1} mode to ~2.4 eV for the 181 cm^{-1} mode). This is exactly what is expected for a distribution of PtBr segment lengths, with the lower-ν_n modes corresponding to longer segments as outlined in the previous section. For the electronic states, the correspondence between shorter segments and larger band-gaps, as implied by the resonance profiles, is also to be expected from simple quantum confinement arguments.

With these results defining parameters, the P-H model has considerable predictive power and can be used to infer the electronic configurations. Taking the 181 cm^{-1} mode as corresponding to a single $Br\text{-}Pt^{III+\delta}\text{-}Br$ unit surrounded by PtCl, one obtains a model parameter set which predicts two $Cl\text{-}Pt^{III+\delta}\text{-}Br$ junction modes at 210 cm^{-1} and 325 cm^{-1}, modes which are indeed observed. A major conclusion of the P-H modeling of the $PtCl_{1-x}Br_x$ system using these parameters is that the electronic healing length across the PtCl/PtBr junctions is extremely short (~1 lattice constant), so that apart from quantum confinement, the electronic and vibrational behavior of the segments is virtually identical to the bulk pure materials.

THE CHLORIDE/IODIDE MIXED SYSTEM

Figure 1 shows resonance Raman spectra of the $PtCl_{1-x}I_x$ system at 20 K, for nominal (solution) I fractions x=0.05 and x=0.2, together with spectra of pure PtCl and PtI for comparison, obtained using Ti:sapphire, HeNe and Ar^+ lasers. Superficially there are many similarities between these spectra and those of $PtCl_{1-x}Br_x$; as in that case, the ν_1 modes of the pure materials are replaced by series of sharp lines, with only the relative intensities, not the mode frequencies, depending on the I fraction. Thus again, PtCl and PtI segments of various lengths seem to be responsible for the complex spectra.

Prominent in the spectra excited at ~1.6 eV is a peak at 116 cm^{-1}. This is a photo-induced defect, which is stable at 20 K but anneals away at room temperature. This defect is unavoidable since it induced by the Raman excitation laser at energies as low as 1.5 eV. From its I concentration dependence, frequency, and lack of a shift upon Cl isotope substitutions, it is clear that this defect resides in the PtI segments.

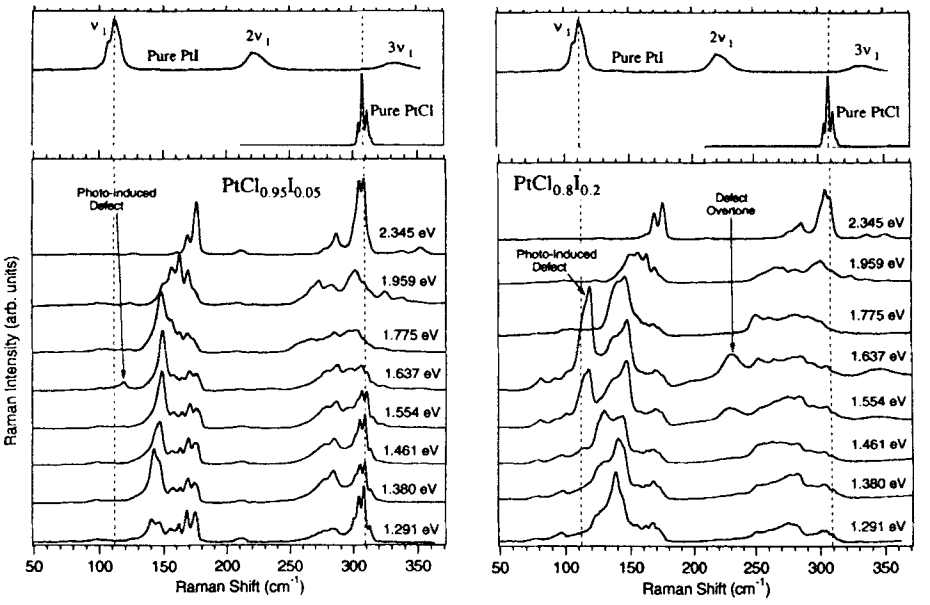

FIGURE 1. Resonance Raman spectra at 20 K, for excitation energies noted at right, of $PtCl_{1-x}I_x$ with nominal (solution) I fractions x=0.05 and x=0.2. Spectra of pure PtI (E_{ex}=1.29eV) and of PtCl are shown at top for comparison.

In contrast to $PtCl_{1-x}Br_x$, the simple correspondence between excitation energy and mode frequency does not rigorously hold for $PtCl_{1-x}I_x$. Furthermore, the entire PtI-like series at low frequency is substantially stiffened relative to pure PtI even at the lowest excitation energies, while the ~300 cm^{-1} PtCl-like modes are softened relative to pure PtCl. The increase in PtI segment frequencies is expected from of the lattice-dynamical effect of finite segment lengths. But the softening of the PtCl segments is surprising, since both the lattice-dynamical finite length effect, and the longitudinal stretching of the PtCl chains observed in x-ray diffraction should lead to higher, not lower, PtCl mode frequencies. This is our first indication that substantial electronic mixing with neighboring soft-CDW PtI segments is occurring, as is predicted by the P-H model for this case. This softening due to the long electronic healing length is quite substantial, since it counteracts two effects which otherwise would raise the PtCl frequency by several cm^{-1}.

The probability that electronic mixing will produce segment-length-dependent bond spring constants, the

complexity of these spectra, and the lack of a simple correlation between frequency and resonance profile for the various modes, makes it impossible to assign observed features to specific segment lengths given only the information shown in Fig. 1. To clarify the correspondences between Raman frequencies and segment lengths, we have performed Cl isotope substitution studies. The basic idea here is that a mode localized on a PtI segment will always have a small but non-negligible fraction of the vibrational amplitude extending into the adjoining PtCl segments. The shorter the PtI segment, the more significant this Cl participation is to the frequency of that segment mode. Thus, upon replacing the natural Cl isotopes (75% ^{35}Cl, 25% ^{37}Cl) with pure ^{37}Cl, short PtI segment modes should display substantial frequency shifts, while longer segments will display smaller changes. Typical results are shown in Fig. 2, together with a compilation of the ratios of the mode frequencies with natural 75% ^{35}Cl to those with pure ^{37}Cl; smaller ratios imply greater Cl character, hence shorter PtI segments. The main result here is that the mode frequencies are not ordered according to decreasing segment length; the highest frequency mode of the PtI-like series (175.7 cm^{-1}) shows no observable Cl isotope effect, indicating substantial PtI segment length. The greatest shift is seen for the 156.4 cm^{-1} mode, indicating this is the shortest PtI segment. Thus we have experimental evidence of segment-length-dependent electronic structures, whose effects outweigh simple lattice-dynamical considerations.

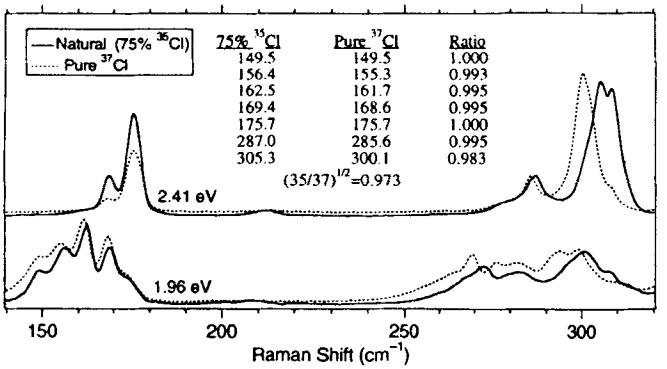

Figure 2. Comparison of RR spectra of $PtCl_{0.95}I_{0.05}$ with 75% ^{35}Cl (natural abundance) and with pure ^{37}Cl.

A more complete picture is obtained by using these experimental results to obtain a parameter set for the P-H model. Figure 3 compares the theoretical Raman spectrum for

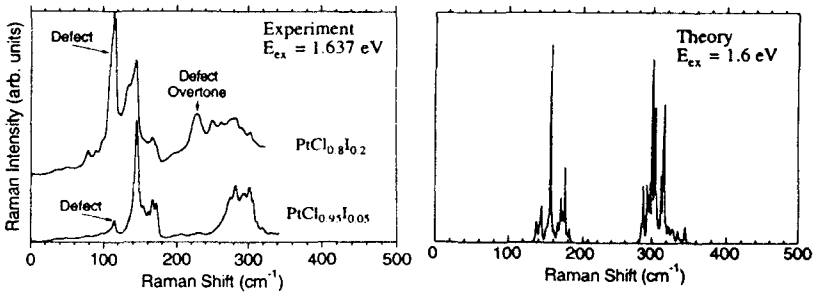

FIGURE 3. Comparison of experimental the calculated (see text) RR spectra of PtClI for excitation energy 1.6 eV.

one excitation energy using our best fit parameter set, with the experimental data. The theoretical spectrum is calculated by summing the results for ten 48-atom $PtCl_{0.8}I_{0.2}$ chains with the I positions determined by a pseudo-random number generator. The parameter set is listed in Table I. See ref. [1,3] for the definitions and the P-H Hamiltonian.

TABLE I. Peierls-Hubbard parameter sets for PtCl and PtI. Units used here are eV for t_0, e_0 and U; eV/Å for α, β, κ_{MM} and K.

	$t_0(eV)$	e_0	α (eV/Å)	β_M	β_X	U_M (eV)	U_X	K_{MX} (eV/Å^2)	K_{MM}
PtCl	1.02	2.12	0.5	2.7	-1.35	1.9	1.3	6.8	2.0
PtI	2.45	2.0	2.53	0.51	-0.255	0.0	0.0	7.42	2.0

One important question resolved by this P-H model fit is whether charge transfer (intrinsic self-doping) occurs across the PtI/PtCl junctions. In the P-H model, this is determined by the PtCl and PtI on-site energies e_0, which, in turn, determine the relative positions of the PtI and PtCl bands. For the pure materials, the on-site energy cannot be experimentally determined because it has almost no effect on the observables (E_{gap}, ν_1, etc.). Early modeling attempts, using the same parameters which previously yielded excellent results for pure PtCl and PtI, predicted that the PtI HOMO should fall above the PtCl LUMO, resulting in electrons being transferred from the PtI to the PtCl segments upon formation of the mixed chains. This parameter set, however, failed to reproduce even the qualitative aspects of the observed Raman spectra. But with a simple adjustment of the e_0 values, sufficient to prevent charge

transfer, the impressive agreement with experiment seen in Fig. 3 is obtained.

The model yields assignments for the various modes, and these show the correct ordering with respect to segment length. The 156 cm^1 mode, for example, is found to correspond to a single I atom isolated in PtCl, consistent with this being the PtI mode with the greatest Cl isotope effect. The peculiar ordering of the short PtI segment modes arises from the discrepancy between the large electronic coherence length of PtI (reflected in its predicted polaron width of ~30-sites) and the short segment lengths terminated by the hard-CDW PtCl; PtI segments this short cannot relax to the bulk ground state configuration. The predicted short coherence lengths of $PtCl_{1-x}Br_x$ (polaron widths 1 and 4 sites for PtCl and PtBr, respectively), in contrast, mean even the shortest segments will resemble the bulk.

Other insights include the assignment of the ~287 cm^1 modes to the complex third type discussed above, with two short PtI segments and the PtCl segment between sharing vibrational amplitude; this explains the mixed I-Cl character revealed by the isotope effect, and the observation that modes in this region form sum bands with both the 149-176 cm^{-1} series of modes (short PtI segments) and the ~305 cm^{-1} PtCl modes.

Finally, the model predicts that, of the possible photo-induced species, hole bipolarons are energetically favored in the PtI segments, with a predicted vibrational frequency of 117 cm^{-1}, in excellent agreement with the observed photo-induced defect.

SUMMARY

The combination of RR spectroscopy and P-H modeling has yielded detailed information on the properties of 1-D heterojunctions and quantum-confined structures in $PtCl_{1-x}Br_x$ and $PtCl_{1-x}I_x$. The striking differences between the two systems are found to arise primarily from the differing CDW strengths and coherence lengths of the constituent materials.

REFERENCES

1. J. T. Gammel, et al., Phys. Rev. B., 45, 6408 (1992).
2. S. P. Love, et al., Synth. Metals, 56, 3335 (1993); Phys. Rev. B., 46, 813 (1992); ibid., 46, 11107 (1993).
3. X. Z. Huang, et al., Solid State Comm., 84, 957 (1992).
4. S. P. Love, X. Z. Huang, et al, Phys. Rev. B., in preparation.